ISSN No:-24562165

Photocatalytic Degradation of Organic Dyes in Aqueous Media Under Visible - Light Irradiation Using Aurivillius – Type Bicrvox Catalysts: Development of New Efficient Photocatalysts for Environmental Applications

Samar W.A.Al-Badani*
Afraah M.A. Alfaatesh
Niyazi A.S. Al– Areqi
Department of Chemistry,Faculty of Applied Science, Taiz Uiversity, Taiz, YEMEN.

Abstract:- A layered perovskite – type designated as BICRVOX.x ($Bi_4Cr_x^{III}V_{2-x}O_{11-3x/2}$) belonging to the Aurivillius family has been synthesized in the composition range of 0.05 ≤ x ≤ 0.20, by the citrate – ethylene glycol sol- gel route followed with the microwave- assisted calcination of resulting xerogels. The present study has been devoted to investigate the effect of Cr(III) doping on phase stability, optical properties and photocatalytic efficiency of Aurivillius type Bi4V2O11. In this investigation, many analytical methods, such as X-ray powder diffraction (XRPD), differential thermal analysis (DTA), thermogravimetric analysis (TGA), Fourier transform- infrared spectroscopy (FT-IR), nitrogen adsorption equipment and UV-VIS spectrophotometry, have been employed. Methylene blue (MB) has been used here as a dye model in aqueous medium to investigate the photocatalytic efficiency of as-prepared BICRVOX.x series under visible- light irradiation. It has been found that the photocatalytic degradation of MB proceeds more rapidly in the compositional range of γ'-phase stabilization, particularly γ'- BICRVOX.15 exhibiting the highest value of apparent velocity constant (kapp = 13.22 × 10-3 min-1), irrespective of the lowest value of its band-gap energy (Eg = 1.64 eV). This unexpected variation may be attributed to the increased crystallinity of γ'-BICRVOX phases (i.e. x = 0.13 and x = 0.15) which interfered with UV-VIS spectrophotometric measurements.

Keywords:- *Photocatalysts , BICRVOX.x , Methylene Blue.*

I. INTRODUCTION

Organic dyes produced from industries and textiles are very dangerous because they cause damage to humans, aquatic organisms and the surrounding environment [1]. In recent years, many efforts have been devoted to the removal of these dyes and other wastes using many physical and chemical techniques. Among these, advanced oxidation processes (AOPs) have been intensively investigated for the photodegradation of dyes in industrial wastewaters. Semiconductor- based photocatalysis has been proven to be potentially advantageous, as it costs less money and does not cause secondary contamination [2]. Among these semiconductors, TiO2 has been widely studied for photocatalytic applications because of its thermal stability, facile preparation, cheapness and the low toxicity [3,4]. However, because of its relatively high band–gap, TiO2 (3.2 eV) is only activated under ultraviolet light irradiation with wavelengths shorter than 387 nm [5]. This leads to severely limits the commercial applications of TiO2 in wastewater treatments. Therefore, many researches have been made to find, design and optimize efficient photocatalysts with maximum absorption thresholds (minimum band gaps) that effectively accelerate the photocatalytic degradation of organic dyes under visible light irradiation.

However, the perovskite- type Bi4V2O11 compound of a layered Aurivillius structure and its metal– doped analogues, acronymized as BIMEVOX.x ($Bi_4Me_x^lV_{2-x}O_{11-(5-l)x/2}$) have attracted a great attention due to their narrow band gap with a potential photocatalytic efficiency under visible light irradiation. It has been proven that these important features of such a type of compounds effectively accelerate the photocataltyic degradation of organic dyes in aqueous media under visible light irradiation [6-8].

As an extension to our previous work on this family of compounds, the current paper aims to investigate the effect of Cr(III) doping on phase stability, optical properties and photocatalytic efficiency of Aurivillius type Bi4V2O11. The present compound can be formulated as $Bi_4Cr_x^{III}V_{2-x}O_{11-3x/2}$ (BICRVOX.x) in the composition range of 0.05 ≤ x ≤ 0.20, which was synthesized by the citrate – ethylene glycol sol- gel route followed with the microwave-assisted calcination of resulting xerogels. However, this study was devoted to provide a clear, convincing evidence to realize an actual relationship between the phase stability, optical properties and visible- light photocatalytic efficiency of BICRVOX.x. Methylene blue (MB) with a molecular formula (C16H18ClN3S.3H2O) [9,10] was employed here as a dye model in aqueous medium to investigate the photocatalytic

ISSN No:-24562165

efficiency of as-prepared BICRVOX.x series under visible-light irradiation.

II. EXPERIMENTAL

A. Preparations of Photocatalyst Samples

➢ *Preparation of BICRVOX.x ($Bi_4Cr_xV_{2-x}O_{11-x/2}$) series ; $0.05 \leq x \leq 0.20$:*

Analytical grade $Bi(NO_3)_3.5H_2O$,NH_4VO_3 and $Cr(NO_3)_3.9H_2O$ were used as starting materials. Stock solutions of the starting materials (0.1 M) were prepared by dissolving an accurately weighed amount of corresponding material in deionized water. A 0.2 M citric acid solution used as chelating agent was prepared in deionized water–ethylene glycol mixture at a volumetric ratio of 3:1. A 0.5 M NH_3 solution was also used for adjusting ph.

The starting materials solutions were mixed at a volumetric ratio of 2:*x*:(1-*x*) = Bi: Cr : V with citric acid solution to form sol solutions. The ratio of citric solution to total metal ions was set at 1.5:1. The pH of resulting sol solutions were adjusted to ~ 7 by adding ammonia solution. The sol solutions were then heated at 80 ◦C under constant stirring for 2 h till forming visible gel. Wet gels were further dehydrated in an oven at 90 ˚C for 12 h to remove excess water and obtain dried xerogels. The xerogel was thoroughly mixed in an agate mortar for further homogenization, then subjected to a microwave-assisted calcination for 5 h in a muffle furnace at temperature of 550 ˚C.

B. Preparation of Dye Solution

The MB aqueous solution was prepared (0.01 M) by dissolving 3.1985 g MB solid into liter (stock solution),1.2 $\times 10^{-5}$ M MB dilute solution prepared by taking dissolving 1.2 ml of the stock solution and diluting it the up to a liter.

C. Structural Characterization

➢ *X-Ray Powder Diffraction*

The X-ray powder diffraction (XRPD) patterns obtained on *a Philips PW 1050/30 X-ray diffractometer* using CuKα radiation (λ= 1.54060 Å), were employed to determine the identity of stabilized phases present and their crystallite sizes and densities. The diffraction beams were collected by a Bragg–Brentano geometry in the range of $^{\circ}10 \leq 2\theta \leq 90$ with an increment of 0.15˚ at a scan time of 1.3 s/increment .The unit cell parameters were refined using an *X'Pert Plus* software program.

The average crystallite size , *D* was calculated from the line broadening using the Scherer equation: $D = 0.89\lambda/B \cos \theta$ where is the CuKα radiation wavelength (λ= 1.54060 Å) , B is the half width of the peak in radians and θ is the corresponding diffraction angle.

D. Thermal Analysis

Differential thermal analysis (DTA) thermograms collected on *a Perkin– Elmer thermal analyzer, or Shiatsu SC-TA 60 Thermal analyzer* were used to investigate the thermal stability range of different phases of the catalyst. A dry sample of the BIMEVOX.*x* oxide (20 mg) was placed in the α-alumina cell and the DTA experiment was run in nitrogen atmosphere. The flow rate of nitrogen was $^{-1}$ ^{o}C min^{-1} from ambient to maintained at 30 ml min with a heating rate of 10 1000ºC. Thermogravimetric analysis (TGA) Thermograms of sample xerogels were obtained at the same conditions.

E. Furrier Transform – Infrared Spectrometry

FT–IR spectroscopy was also employed to investigate the decomposition of xerogels. Transparent pellets were prepared by diluting the treated xerogels with KBr to 1.5 w/w %, which were ultimately pressed under isotactic pressure of 240 MPa. The FT–IR spectra of selected compositions calculated at various temperatures were recorded on *a Perkin Elmer 1 spectrophotometer* in the transmittance mode over a wave number range of 4000 – 400 cm^{-1}.

F. Optical Characterization

The optical band-gap energy (E_g) of as-sintered samples of the photocatalyst was estimated using the UV–VIS spectra. The UV–VIS .Spectral data were collected on *a Shimadzu Scan UV–VIS spectrophotometer (UV-2450)* at room temperature in the wavelength range 200–800 nm. The values of direct band-gap energy were determined by extrapolating the straight portion of the absorption edge to (absorbance) A = 0 point [5,6]. The wave length of the band–edge (λg) were used to calculate E_g using equation (1):

$$E_g(eV) = \frac{1240}{\lambda_g(nm)} \quad (1)$$

G. Adsorption Measurements

Surface area measurements of BIMEVOX.*x* photocatalyst series were performed using the nitrogen adsorption–desorption isotherm at 77 K on *an Autosorb1 (Quantachrome) adsorption apparatus*. The adsorption data were collected in the nitrogen partial pressure range of $0.01 \leq (P/P_o) \leq 0.99$. The specific surface area (S_{BET}) expressed in $m^2g^{-1}$was calculated by the BET method.

H. Kinetics of Photocatalytic Degradation

MB dye solution 250 ml of 1.2×10^{-5} M at pH ∼10.0 was transferred in to a 450 ml photoreactor, equipped with water refrigeration and magnetic stirrer. Accurately weighed 100 mg of the BICRVOX.*x* photocatayst was dispersed in the dye solution. The resulting suspension was then magnetically stirred in the dark for 40 min to reach the adsorption–desorption equilibrium. A 300-W xenon lamp, located beyond an optical glass cut-off filter was used as the visible-light source with wavelengths greater than 400 nm. The irradiation source was located at 25 cm above the surface of liquid in the photoreactor. The temperature of reaction system was kept at 25ºC using flowing cool water in order to prevent the thermal catalytic reaction effect. At equal time intervals of irradiation (10 min), 5 ml aliquot of the reaction mixture was withdrawn from the photoreactor and filtered to separate the catalyst residues. The dye concentration versus irradiation time was determined by measuring the maximum absorbance at λ_{max}= 661 nm using *a Shimadzu UV–vis spectrophotometer(UV-*

2450). The photocatalytic activity of the BIMEVOX.*x* catalyst as a function of composition for the dye photodegradation were investigated using the pseudo-first-order kinetic model:

$$\ln\left(\frac{C_t}{C_0}\right) = -k_{app}t \qquad (2)$$

➢ *Where*

C_o and C_t are the initial concentration and concentration at irradiation time, t of MB dye solution, respectively and k_{app} denotes the apparent first-order rate constant.

However this model was graphically represented as ln (A_t/A_o) vs. t plots.

III. RESULTS AND DISCUSSIONS

A. TGA–DTA Thermograms of BICRVOX.10 Xerogel

TGA–DTA curves of BICRVOX.*10* xerogel are presented in (Fig.1), which generally shows obvious two–step thermal degradation, starting from ~ 85ºC and extending upto 418 ºC .Two thermal events are accompanied with the overall decomposition, which can be seen in DTA curves: an endothermic peak at ~119 ºC and a sharper exothermic peak is noticed below ~361ºC. However, the first weight loss of the thermal degradation (~10.7%) , corresponding to the endothermic peak is attributed to the elimination of physically adsorbed ammonia and water from the xerogel. It is also possible that free ammonium citrate is partially decomposed in this step [7,8].The second weight loss (~39.5%) in the temperature range 200 – 420ºC, corresponding to the exothermic peak is associated with a fast decomposition and decarbonization of chelating citrate [9]. Moreover, this step involves the oxidation of excess ammonium nitrate present in the xerogels.

It is also important to point that the small endothermic peaks noticed in DTA curves (Fig.5)at temperatures above 440 ºC without any corresponding mass loss in TGA curves are correlated with the occurrence of phase transition in the BICRVOX system.

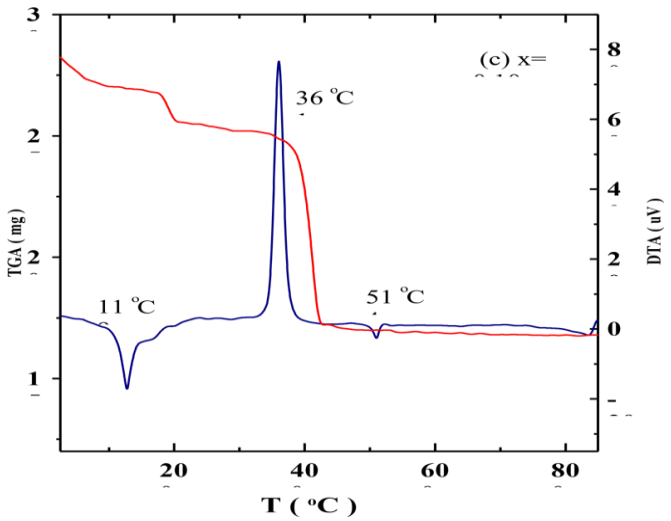

Fig.1: TGA – DTA curves of BICRVOX.*10* xerogel .

B. FT–IR Spectra of BICRVOX.15 Xerogel

Thermal decomposition of BICRVOX xerogels has been further studied by FT– IR spectroscopy. For the sake of comparison with TGA-DTA results,(Fig.2) shows

FT–IR spectra of BICRVOX.*15* xerogel collected immediately after three hours of calcination at different temperatures. The dry xerogel is characterized by absorption bands associated with precursor metal complex and excess salts [9] bands at 1415 and 1610 cm^{-1} are characteristics of stretching and vibration modes of carboxylate group. A band at ~ 1750 cm^{-1} is ascribed to C=O stretching . Vibration modes of M-O bond are found at 1060 and 520 cm^{-1} are attributed to V-O and Bi-O bonds respectively. In addition, C-O stretching, C-H deformation and O-H bending modes are subsequently noticed at ~1240, 1185 and 1008 cm^{-1}. However, a high–frequency band at ~ 2580 cm^{-1} is characteristic of stretching mode of O-H vibration, whereas a broad band that appears at ~ 3470 cm^{-1} signifies the presence of water and excess ammonium salts. There is an evidence for the existence of nitrates in the dry xerogel due to which bands are apparent at ~ 1390 and 865 cm^{-1}. It can be noted that the general features of FT–IR spectrum described for the dry xerogel are entirely preserved with increasing calcination temperature upto 250 ºC. It is observed that most of the absorption bands shift towards low–frequency side of the spectrum with remarkable disappearance of some bands in the xerogel calculated at 300ºC. This is attributed to the decomposition of ammonium citrate and nitrate from the xerogel. It is also observed that the remaining bands ascertained to the precursor metal complex widen as the calcination temperature increases. Importantly, a broad spectrum is noticed in lower frequencies for the powder calculated at 550ºC, which is assigned to the oxide, BICRVOX and is similar to what have been reported earlier for other BIMEVOXes [10,11]. It is noteworthy that the bands in the frequency regions ~1010 – 820 cm^{-1} and ~640–520 cm^{-1} are attributed to asymmetric stretching and deformation modes associated with vanadate anion in the perovskite–like sheets, bands which are noticed at ~723 and 431 cm^{-1} are ascribed to the symmetric stretching (V-O) and (Bi-O), respectively [10].

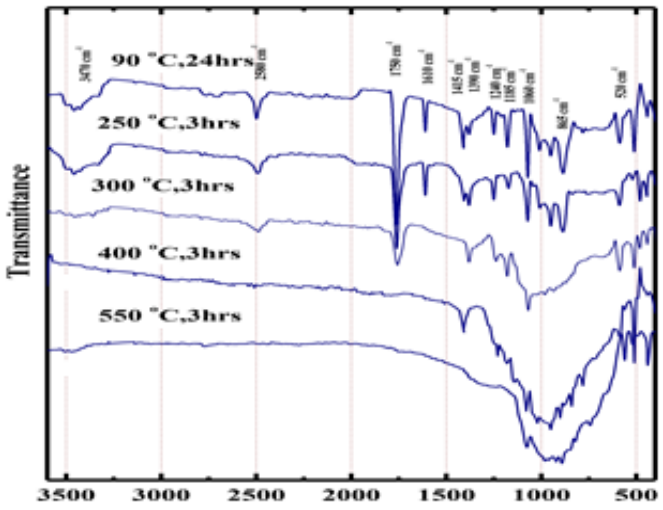

Fig 2 FT–IR Spectra of BICRVOX.*15* Zerogel Calculated at Different Temperatures for 3 Hours.

ISSN No:-24562165

C. X. Ray Crystallography

The variation in XRPD patterns of as-synthesized BICRVOX.*x* photocatalyst series as a function of Cr substitution is illustrated in Fig. 4. The diffraction patterns for the catalyst compositions $x = 0.05$ appear to be identical to the characteristic α-phase. This is clearly evidenced by the existence of doublet sublattice peak (022) and (220) at $2\theta \sim 32^{\circ}$,and the doublet sublattice peak (026) and (606) at $2\theta \sim 46.2^{\circ}$, which are characteristic to the monoclinic symmetry with a space group, *Ab2* [12], The diffraction patterns for the catalyst compositions $x = 0.07$ and 0.10 appear to be identical to the characteristic β-phase diffraction pattern which is clearly evidenced by the existence of doublet sublattice peak (020) and (200) at 2θ 32◦,and singlet peak (220) at $2\theta \sim 46.2^{\circ}$, which are characteristic to the orthorhombic symmetry with a space group, *Acam* [6]. The diffraction patterns for the catalyst in the compositional range $0.10 < x \leq 0.20$ appear to be identical to the characteristic γ '-BICRVOX phase with a space group *I4/mmm*, which is definitely clear from the appearance of a singlet sublattice peak indexed as (110) at $2\theta \sim 32^{\circ}$ [13].

Values of unit cell refinement, average crystallite size and crystallographic density evaluated by fitting diffraction patterns are listed in Table 1. It is clear that the incorporation of Cr^{+3} ions into the $Bi_4V_2O_{11}$ compound causes a dramatic increase in the unit cell dimensions (particularly a and c) , accompanied by the same trend in the overall cell volume. The density strongly depends on the initial crystallite size. However, a slight lowering in the particle size accompanied with the increase of density can be observed as the Cr substitution increases. This trend is in a good agreement with the variation of unit cell parameters, reflecting the positive contribution of Cr substitution to the overall lattice expansion as a consequence of the incorporation of Cr (lll) dopants with a larger ionic radius (0.755 Å) into the perovskite vanadate layers in the place of pentavalent vanadium sites(0.68 Å) [14,15].

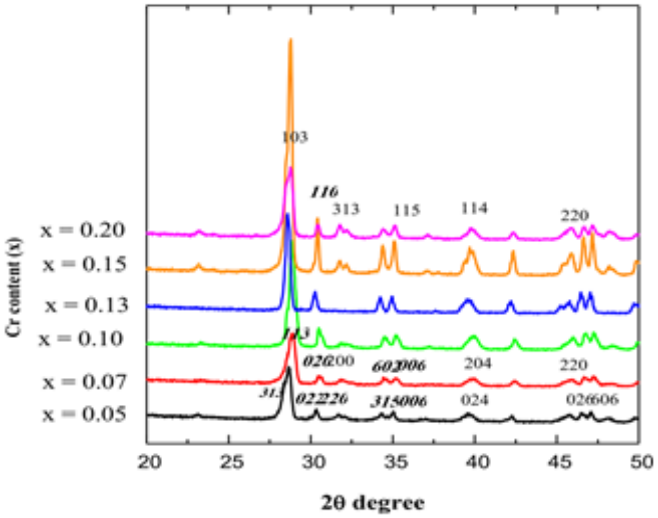

Fig 3 XRPD Patterns of as–Synthesized BICRVOX.*x* Photocatalysts.

D. Differential Thermal Analysis

Thermal stability of the BICRVOX.*x* system along with the estimated values of enthalpy at the onset temperature of phase transitions are presented in DTA thermograms (Fig.6.) The two characteristic endothermic peaks clearly seen for the photocatalyst for the compositions with $x = 0.05$ on heating run are attributed to the consequent α→ β and β → γ transitions. However, the BICRVOX.*07* sample shows a single endothermic peak at 482.73◦ C assigned to the β → γ transition ,while the occurrence of incommensurate → commensurate, the β-BICRVOX.*10* sample shows a single endothermic peak at 466.3◦C assigned to the β → γ transition, where γ′→ γ transition is detected in the compositional range $x \leq 0.10$.

It is interesting to note that the variation of transition temperature, T_t with Cr substitution shows a remarkable increase indicating an increased ordering of oxygen vacancies in the perovskite vanadate layers [16,17], This can also be correlated with the lattice expansion as revealed earlier in XRPD results. Furthermore, the transition enthalpy, ΔH_t generally decreases with increasing Cr dopant content. It is clearly evident that the remarkable drop of ΔH_t along compositions with $x \geq 0.13$ is indicative of higher thermal stability of γ′-BICRVOX.x photocatalysts [18,19] .

Table 1 Refined unit cell parameters, phase stabilizations, average crystallite sizes and crystallographic densities of as– prepared BICRVOX.x series.

	Unit Cell Rsparamete						Phase Stabilization	Crystallite Parameters
x	A (Å)	B (Å)	C (Å)	V(Å^3)	Phase	Space Group	Average Crystallite Size (Mm)	Crystallographic Density, Dxrpd (G Cm_3)
0.05	5.533	5.628	15.281	475.84	□	Ab2	3.91	6.87
0.07	5.539	5.613	15.323	476.39	□	Acam	3.87	6.74
0.10	5.582	5.578	15.591	485.45	□	Acam	3.88	6.79
0.13*	5.616	–	15.898	501.41	Γ'	I4/M Mm	4.02	6.84
0.15*	5.632	–	15.887	503.93	Γ'	I4/M Mm	3.93	6.78
0.20*	5.651	_	15.905	507.91	Γ'	I4/M Mm	4.17	6.82

ISSN No:-24562165

E. Surface and Optical Properties of BICRVOX.X Photocatalysts

Fig .5 shows UV- VIS absorption spectra of the BICRVOX.*x* system for various compositions. The absorption edges of some compositions in the BICRVOX.*x* system are found to be lower than that of the pure $Bi_4V_2O_{11}$compound as reported earlier [20]. This suggests that the doping strategy by aliovalent metal ions plays a significant role in improving the photoabsorption and photocatalytic activities of $Bi_4V_2O_{11}$. It is clearly observed that the compositions with $x = 0.13$ and $x = 0.15$ have higher absorbances than the other compositions. The estimated values of E_g along Fig .5 : DTA thermograms of as–synthesized BICRVOX.*x* photocatalysts. with their corresponding correlation factors (R^2) are summarized in Table.2. It can be observed that the band-gap energy increases with increasing Cr content upto $x = 0.10$ and beyond it decreases to ~ 1.851 eV for $x = 0.13$, and ~ 1.64 eV for $x = 0.15$. Thereafter, it sharply increases to a ~ 2.68 eV for x =0.20. The unexpected reduction of E_g value with otherwise increasing Cr content at intermediate dopant concentrations, i.e., $x = 0.13$ and 0.15, may be attributed to the apparent increased relative crystallinity of BICRVOX powder, particularly for the composition $x = 0.15$, which can be evidenced by the XRD results.

Where $I_{(103)}^{x=0.15}$ and $I_{(103)}^{x=0.2}$ are the intensity of sublattice peaks indexed as (103) in the XRD patterns of γ′-BICRVOX.*15* and γ′-BICRVOX.*20* taken as the sample and standard reference , respectively. It is clear that remarkably higher intensities of some sublattice peaks characteristic to the γ′-tetragonal symmetry ,i.e.,(103) and (110) can be observed in XRD pattern of BICRVOX.*15* sample relative to that of standard BICRVOX.*20* sample (fig.4). It is likely that the perfect distribution of Cr dopants within the highly crystalline BICRVOX photocatalyst may result in the development of mirror-like faces of the crystallites, leading to scatter some of incident radiation beam , and consequently dispatching of absorbing energy during the spectrophotometric experiments for recording the UV-VIS absorption spectra of BICRVOX.x series (Fig 6).

The values of special surface areas obtained by BET isotherm model (S_{BET}) are also listed in Table 2. Almost appreciably equal, high surface areas were found for all investigated compositions with acceptable R^2 values of estimation.

The interesting point to be emphasized here is that the adsorption of MB dye onto the perovskite vanadate layers is effectively enhanced by the columbic interaction between positively charged nitrogen atoms of the dye molecules and oxygen vacancies or atoms of BICRVOX.*x* photocatalysts. This indicates that the BICRVOX.*x* photocatalyst system with its layered Aurivillius-type structure can offer a high specific surface area with sufficient number of active sites available for the dye adsorption, and consequently favorable for enhancing the photocatalytic performance.

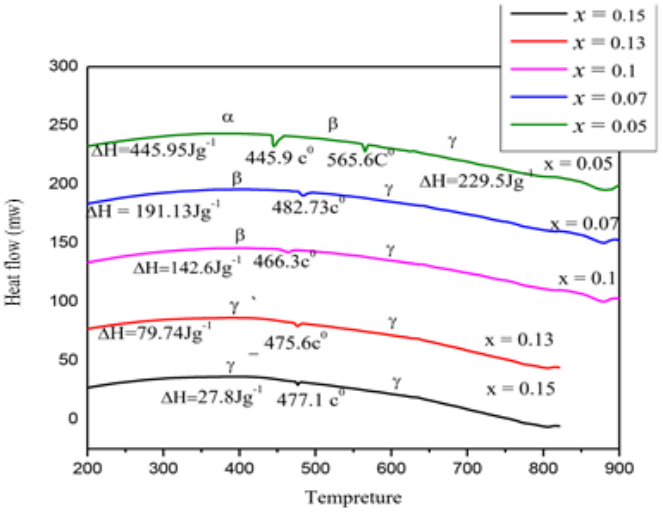

Fig 4 DTA Thermograms of as–Synthesized BICRVOX.*x* Photocatalysts

F. Photocatalytic Efficiency of BICRVOX.X Photocatalyst Series

Photocatalytic efficiency of as - synthesized BICRVOX.*x* compositions was investigated through the degradation of MB dye solution under visible-light irradiation using equally weighed amounts of BICRVOX.*x* photocatalysts. Fig.4.6 depicts the pseudo-first-order kinetic representation of the photocatalytic degradation of MB dye at varying BICRVOX.*x* compositions. The red - colored lines presented in the figure show the quality of line- regression fitting to the experimental data. The calculated values of the apparent rate constants (k_{app}) as a function of Cr content, along with the corresponding correlation factors (R^2) are illustrated in Table .2. The variation in the photocatalytic degradation rates exhibits two local minimums; once for stabilized β- phases (*i.e.*, $x = 0.10$), and another for stabilized γ'- phases (*i.e.*, $x = 0.20$). Despite, the highest value of S_{BET} for βBICRVOX.*10* Photocatalyst ,*i.e.* the highest surface area of the catalyst available for the adsorption of more dye molecules, the phocatalytic degradation is found to go slowing down reaching it lowest level (Kapp = 6.91×10^{-3} min^{-1}) , which can be which can attributed only to the maximum E_g value estimated for $x = 0.10$ (~2.65 eV).This suggests that the electronic contribution is much more greater than the contribution of adsorption coverage to the photocatalyst efficiency of the BICRVOX.*x* system. For γ'BICRVOX.*20* photocatalyst the phocatalytic degradation is found to go slowing down(Kapp = 6.82×10^{-3} min^{-1}) which can be attributed only to the maximum E_g value estimated for $x = 0.20$ (~2.68 eV), Such otherwise slowing down in the photocatalytic degradation of MB dye with the decreased E_g and increased S_{BET}, is likely associated with some vacancy-ordering phenomena occurring in the pervoskite vanadate layers. This can be explained by the fact that at these values of Cr substitution , increased oxygen vacancies are created more preferentially at the apical of perovskite vanadate layers other than at the equatorial planes. Such apical vacancies are thought to be inactive sites for the dye adsorption which may be attributed to the steric hindrance caused by the alternating bismuthate layers sandwiching between the perovskite vanadate layers, and thereby slowing down the photocatalytic degradation reaction [8].

ISSN No:-24562165

It is interesting to note that the photocatalytic degradation of MB dye proceeds more rapidly in the compositional range of γ'-phase stabilization, particularly γ'-BICRVOX.*15* exhibiting the highest k_{app} value that is found to be matched well with its lowest value of E_g. This suggests that the visible- light photocatalytic activity of the BICREVOX.*x* system is greatly enhanced upon an increasing creation of oxygen vacancies at the equatorial planes of perovskite vanadate layers. The optimal, fully disordered equatorial vacancies responsible for the γ'-phase stabilization [21] play a significant role in generating an electron trap under the CB to narrow band gaps, restraining the recombination of photogenerated holes and electrons and thereby improving the visible-light photocatalytic activity of γ'-BICRVOX.*x* phases.

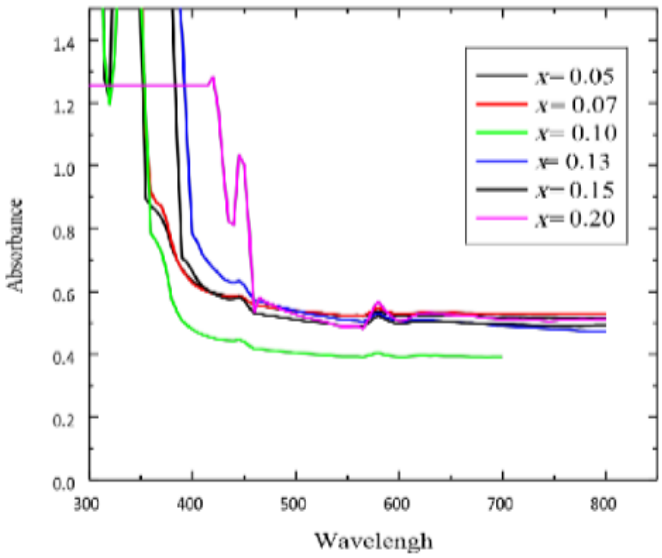

Fig 5 UV–VIS Absorption Spectra of the BICRVOX.x Photocatalysts

The mechanism suggests that MB dye molecules are first adsorbed onto the perovskite vanadate layers as a result of a columbic interaction between positively charged nitrogen atoms of the dye and equatorial oxygen vacancies or atoms. Under visible- light irradiation, the adsorbed MB molecule is then electronically excited to appropriate singlet or triplet states [28]. This photophysical process is accompanied by an electron ejection from the excited dye molecule onto the CB, leaving behind a cationic dye radical (MB•+) that undergoes degradation to yield mineralization products. It is interesting to mention here that O2 molecule adsorbed on the BICRVOX surface or dissolved in water is reduced by the electrons photogenerated in the CB and OH− or H2O can be oxidized by the photogenerated holes of the VB, together producing a very strong oxidizing agent, hydroxyl radicals (OH•), whose standard redox potential is + 2.8 V, which can oxidize most dye molecules to mineral end products.

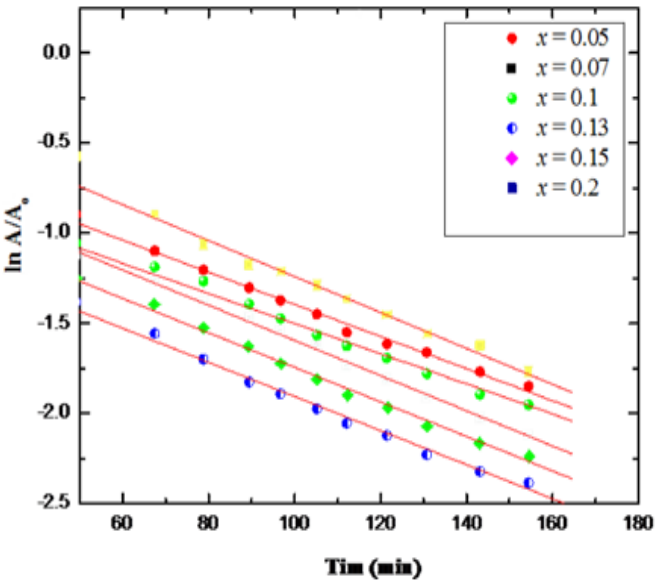

Fig 6 Photocatalytic Activities of the BICRVOX.x Catalyst Series for the Degradation of MB Dye Solution Under Visible Light Irradiation.

Table 2 Estimated Special Surface Area, Band–Gap Energies and Photo degradation Rate Constants of MB Dye by BICRVOX.x Series Under Visible Light Irradiation.

X	Specific Surface Area And Dye Equilibrium Adsorption		Optical Band–Gap Energy		Photocatalytic Activity	
	SBET ($M^2 G^{-1}$)	R^2	E_g (Ev)	R^2	Kapp ×10–3 (Min^{-1})	R^2
0.05	0.39	0.9994	2.21	0.9036	7.88	0.9984
0.07	0.31	0.9990	2.52	0.9505	8.94	0.9862
0.10	0.36	0.9986	2.65	0.9110	6.91	0.9874
0.13	0.28	0.9992	1.851	0.9362	8.96	0.9895
0.15	0.26	0.9993	1.64	0.9076	13.22	0.9108
0.20	0.23	0.9988	2.68	0.9837	6.82	0.9877

ISSN No:-24562165

IV. CONCLUSION

The BIMEVOXes are a large family of Aurvillius-structural type of compounds that can be derived by the partial substitution of V in the parent compound by a variety of cautions almost irrespective of their ionic radius.

This work has been devoted to study the photocatalytic degradation of MB dyes in aqueous solutions under visible - light irradiation using Aurivillius– type BIMEVOX catalysts, which can be formulated as $Bi_4 Me_xV_{2-x}O_{11-[(5-l)x/2]-\delta}$, where $Me = Cr^{3+}$.

These systems have been synthesized by the sol-gel ethylene glycol - citrate followed by the conventional heating and/or the microwave – assisted calcination over particular composition ranges below which all the possible compositionally dependent phases can be noticed. Many advanced techniques have been employed in this investigation, such as X–ray powder diffraction, thermal analysis (TGA/DTA), BET adsorption isotherms, FT–IR, and Shimadzu Scan UV–Vis spectrophotometer (UV-2450). It has been found that the stabilization of α–and β–polymorphs to room temperature, with respect to Cr takes place remarkably at a low dopant concentration similar to that in other BIMEVOXes The unexpected variation in the band – gap energy of BICRVOX.*x* system with content may be attributed to the increased crystalinity of γ'-BICRVOX phases(*i.e.x* = 0.13 and *x*= 0.15) affecting the UV – Vis spectrophotometric measurements.

It is interesting to note that the photocatalytic degradation of MB dye proceeds more rapidly in the compositional range of γ'-phase stabilization, particularly γ'BICRVOX.*15* exhibiting the highest k_{app} value that is found to be matched well with its lowest value of E_g.

In the light of the conclusion withdrawn, a general reaction mechanism of the photocataiytic degradation of MB dye by BICRVOX.*x* catalyst systems were proposed to illustrate the correlation between the Aurivillius crystal structure of these photocatalysts and their photocatalytic efficiency.

It can be concluded here that BICRVOX.*x* exhibit considerably efficient photocatalysis. Thus, they are strongly recommended as promising photocatalysts for visible-light photodegradation of organic dyes or contaminants present in the the industrial wastewater.

Finally, hope this research work finds sound and motivation among research workers in the field to make further attempts in extending our work via either selecting other metal ions as dopants or applying some other preparation or fabrication techniques in order of enhancing the photocatalytic degradation efficiency.

REFERENCES

[1]. L.Xu, G. Wang, F. Ma, Y. Zhao , Nan Lu , Yihang Guo and X.Yang, Photocatalytic degradation of an aqueous sulfamethoxazole over the metallic silver and Keggin unit codoped titania nano composites, Appl.Surf. Sci., 258 (2012) 7039.

[2]. R. H. Schirmer , H.Adler , M. Pickhardt, E.Mandelkow, methylene blue, Neurobiology of Aging.,32(2011)2.

[3]. A. Miclescu and L. Wiklund, Methylene blue, an old drug with new indications, Jurnalul Român de Anestezie Terapie intensive,17(2010)35.

[4]. D. J .Eaglesham, C. J. Humphreys, N. Mc, N.Alford, W. J. Clegg, M. A. Harmer, J. D. Birchall, High temperature superconducting ceramics, Mater. Sci. Eng., B,1 (1988) 229.

[5]. Y. Zheng, F. Duan, M.Q. Chen and Y. Xie , Synthetic Bi2O2CO3 nanostructures: Novel photocatalyst with controlled special surface exposed, J. Mol. Catal. A 317 (2010) 34 – 40.

[6]. E.J. Li, K. Xia, S.F. Yin, W.L. Dai, S.L. Luo, C.T. Au, Preparation, characterization and photocatalytic activity of Bi2O3– MgO composites, Mater.Chem. Phys. 125 (2010) 236–241.

[7]. H Lin , Ch.Ding , K .Sato,Y.Tsutai, H.Ohtaki, and M . Iguchi , C. Wada, T. Hashida, preparation of and SDC electrolyte thin films on dense and porous substrates by modified sol- gel route , Mater. Sci.Eng.B ,148(2008)73

[8]. A.Al-Alas, S.Beg, N.A.S.Al-Areqi and S.Hafeez, Influence of microwave - assisted calcination on structural properties and oxide – ion performance of layered– pervskite γ-BIMEVOX solid electrolyte synthesized by ethylene glycol–citratesol–gel route ,J.Euro.ceram.Soc.,33,

[9]. S.Beg, A.Al-Alas, and N. A.S. Al-Areqi, Layered Aurivillius compound : synthesis,characterization, and electrical properties, J.Alloys Compd.,504 (2010) 413.

[10]. S.Beg , N.A.S. AL-Areqi , and S.Haneef , Study of phase transition and ionic conductivity changes of Cd – substituted Bi4V2 O11- δ , Solid State Ionics, 179(2008) 2260 .

[11]. S.Beg , N.A.S. AL-Areqi, S.Hafeez , and A. Al-Alas, Improved structural and electrical properties of nickel and aluminum co-doped Bi4V2O11 solid electrolyte, Ionics , 21 (2015) 421.

[12]. F.Krok, I.Abrahams, A.Zadrozna, M.Małys, W.Bogusz, J..G.Nelstrop and A.J.Bush, Electrical conductivity and structure correlation in BIZNVOX, Solid State Ionics,119(1999)139.

[13]. N.A.S. Al-Areqi and S. Beg, Phase transition changes in Bi4CexV2−xO11−(x/2)−δ system ,Mater. Chem. Phys, 115 (2009) 5.

[14]. R.D. Shannon and C.T.Prewitt, Effective ionic radii in oxides and fluorides, Acta Crystallogr.B , 25 (1969) 925.

[15]. R. D. Shannon , Revised effective ionic radii and systematic studies of interatomic distances in halides and chalcogenides, Acta Cryst A32, (1976)751.

[16]. E. Pernot, M. Anne, M. Bacmann, P. Strobe1, J. Fouletier, R.N. Vannier, G.Mairesse, F. Abraham and G. Nowogrocki, Structure conductivity of Cu and Ni-substituted Bi4V2O11 compounds, Solid State Ionics, 70–71 (1994) 259.
[17]. M. Alga, A. Ammar, R. Essalim, B. Tanouti, A. Outzourhit, F. Mauvy, and R. Decourt, Study on structural, thermal, sintering and conductivity of Cu-Co doubly substituted Bi4V2O11 ,Ionics, 11 (2005) 81.
[18]. A. Watanabe, K. Das, Time-dependent degradation due to the gradual phase change in BICUVOX and BICOVOX oxide-Ion Conductors at temperatures below about 500°C, J.Solid State Chem. 163 (2002) 224 .
[19]. W. Wrobel, I. Abrahams, F. Krok, A. Kozanecka, M. Malys, W. Bogusz, and J.R. Dygas, Solid State Ionics , 175 (2004) 425.
[20]. I.K. Konstantinou, T.A. Albanis, TiO2-assisted photocatalytic degradation of azo dyes in aqueous solution: kinetic and mechanistic investigations: A review, Appl. Catal. B: Environ. (2004)1.
[21]. M. Malys, I. Abrahams, F. Krok, W. Wrobel, and J.R. Dygas, Solid State Ionics , 179 (2008) 82.
[22]. C. Bauer P. Jacques, A. Kalt, Photooxidation of an azo dye induced by visible light incident on the surface of TiO2, J. Photochem. Photobiol. A, 140 (2001) 87.